

CHARACTERISTICS OF PRECIPITATION STRUCTURE OF TYPHOON NARI (2001)

Ben Jong-Dao Jou 周仲島 and Chien-Wen Yen 顏健文

Department of Atmospheric Sciences, National Taiwan University, Taipei, Taiwan

ABSTRACT

In this study, the precipitation structure of Typhoon Nari (0116) before and after landfall is examined using the reflectivity data collected by Doppler radar in northern Taiwan and TRMM TMI and PR data. Pronounced precipitation structure changes were identified. The intensification of precipitation in the inner core was observed and this phenomenon could be traced back 5 hours before landfall. The maximum rainfall was shifted from motion right to motion front and then to motion rear portion. The change of the asymmetrical precipitation structure can be crudely attributed to the effect of Taiwan topography. Very low brightness temperature observed by 85GHz TMI and deep and intense reflectivity observed by PR all suggest the existence of severe convective activity and is closely related to the heavy rain after Nari made landfall.

1. Introduction

Heavy rainfall and flash flood produced by landfall typhoons is one of the biggest natural disasters in Taiwan. Not only human lives and personal property were severely demolished, but also the societal stability and sustainability were greatly threatened. To understand and predict heavy rainfall and flash flood caused by landfall typhoons has become the most urgent challenge the meteorological community in Taiwan to face. The island wide Doppler radar network has been completed in 2001 and four NEXRAD type S-band Doppler radars are in operation since then. In this study, the precipitation structure of Typhoon Nari (0116) before and after landfall is

investigated using the reflectivity data collected by Wu-Feng-Shan radar (northern Taiwan). Typhoon Nari made landfall at northern Taiwan on Sept. 16, 2001. Its slow movement and associated heavy rainfall and flash flood caused many fatality and more than 3B US\$ property damages. In addition to the NEXRAD data, TRMM TMI and PR data were also used to study the precipitation structure changes of Nari during landfall period.

2. Azimuth-mean reflectivity display

The space and time variations of precipitation of Nari are examined by restructuring the reflectivity data with radar site as

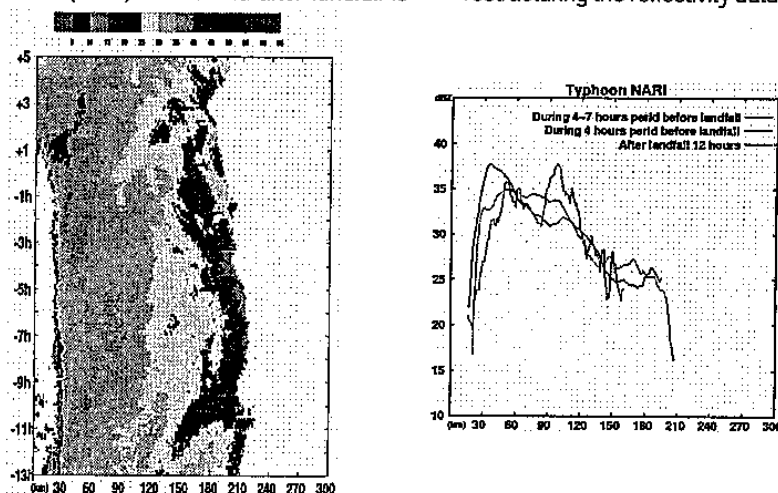


Fig. 1. Hovmöller diagram of 4 km height azimuth mean reflectivity (in dBZ) of typhoon Nari. The abscissa is distance in km from the storm center and the vertical coordinate is time in hours before (-) and after (+) the storm made landfall (left). The azimuthally-mean reflectivity profiles 4-7 hours before landfall, 0-4 hours before landfall, and 12 hours after landfall, respectively. Typhoon Nari made landfall in northern Taiwan on 1340UTC September 16, 2001 (right).

origin into cylindrical coordinate with storm center as origin. In Fig.1, the Hovmoller diagram, total 18 hours, 13 hours before landfall and 5 hours data after landfall, of azimuthally-mean 4 km height reflectivity field is given. Each bin (1 km resolution) of reflectivity was calculated by averaging data azimuthally and the time interval of observation was 6 minutes. The figure shows the precipitation area of typhoon Nari extended 200 km in radius. The eye region with echo less than 10dBZ was about 20 km wide. Significant precipitation occupied region from 20 km to 110 km with mean reflectivity value larger than 30 dBZ. No distinguished echo peak was observed when the storm was still far away from the island. Reflectivity larger than 35 dBZ scattered between 40-110 km range in an earlier time and became to concentrate into eye wall region, i.e., 30-60 km range, however, when the storm moved closer to the island. The near center precipitation intensified significantly during landfall period. The eye contracted and filled with precipitation after the storm made landfall.

For a crude quantitative analysis, we divided the precipitation distribution of Nari into three annular rings (e.g., $r < 100\text{km}$, ring A, the inner core region; $100\text{km} < r < 200\text{km}$, ring B, the outer region 1; and $r > 200\text{km}$, ring C, the outer region 2; respectively), the area-weighted precipitation (using $Z=300R^{1.4}$ to convert mean reflectivity into rainfall rate) can be estimated respectively. The area-weighted precipitation total in the inner core region was almost the same as that in the outer region while the storm was still 12 hours before landfall. It was observed that the precipitation total of the inner core increased gradually and the

outer core decreased at about the same rate while the storm approached to the island. At landfall, the area-weighted precipitation total in the inner core possessed more than 75% of rainfall for the whole storm system. Concentration of precipitation into the inner core of the storm is an indicator for an intensifying storm (Rodgers et al. 1994) and this is the case Nari was experienced in this period. However, it is interesting to note that at about one hour before landfall, the inner core precipitation total increased at a rate about four times faster than that previously had. This abrupt increase of precipitation in the inner core of the storm seems to suggest the pronounced influence of topography on enhancing the precipitation of landfall typhoons.

3. Asymmetrical structure of precipitation

The change of the asymmetrical structure of precipitation of Nari during its landfall period is examined. In this study, the quadrant-averaged rainfall rates divided according to vertical wind shear vector is calculated. At about 13 hours before landfall, the mean (200- 850 hPa) vertical wind shear was directed to NE and the storm moved SW, the maximum rainfall rate occurred in upshear left and right front of movement. The maximum rainfall rate moved to the forefront of movement during landfall. 5 hours after landfall, the maximum rainfall rate occurred at the right rear quadrant of movement. The pronounced effect of vertical wind shear on the asymmetrical structure of precipitation of tropical cyclone has been recognized (Corbosiero and Molinari 2002).

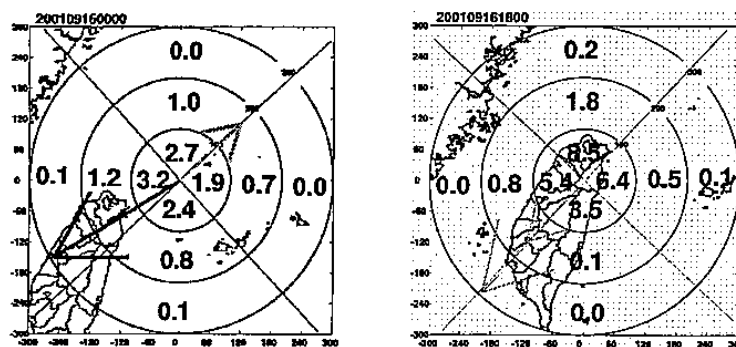


Fig.2. Displays of annular-quadrant mean rainfall rates (unit in mmh^{-1}) of typhoon Nari before (left) and after (right) landfall. The long arrow indicates the movement of the storm and the short arrow indicates the 200-850 hPa mean vertical wind shear direction.

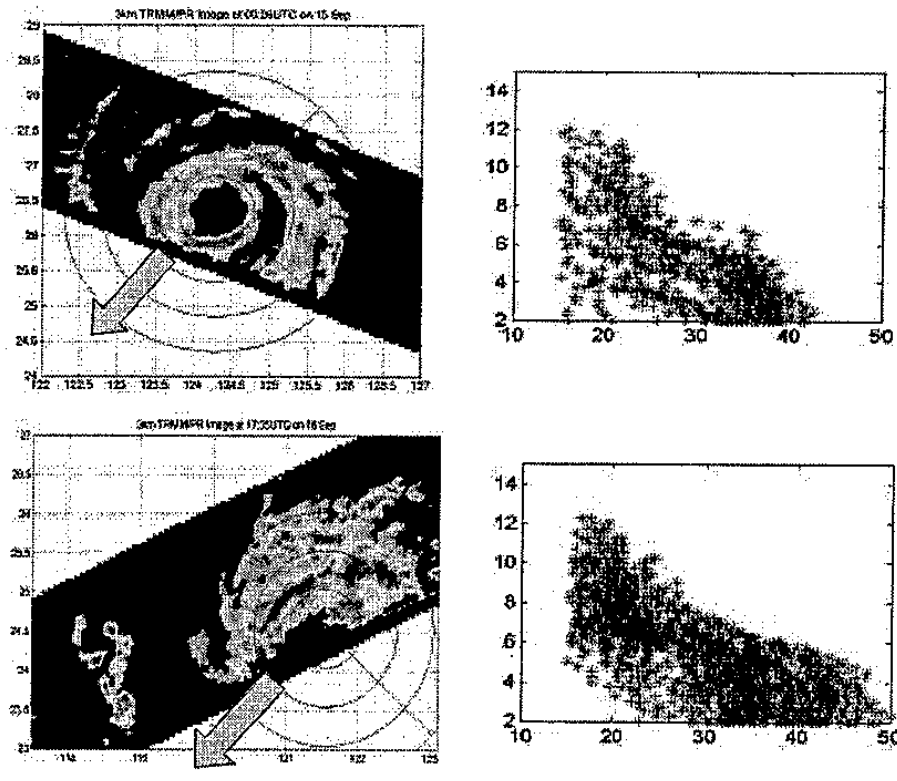


Fig.3. TRMM PR 3 km height reflectivity images and vertical profiles of reflectivity of convective precipitation in motion right front quadrant of Typhoon Nari (a) before landfall, 2001/9/15/0028UTC, and (b) after landfall 2001/9/16/1739UTC.

In Nari case, the 200-850hPa mean vertical shear calculated based on Hanley et al. (2001) was very weak and smaller than 1 m/s for the whole period, and the effect should be minimal. On the other hand, the moving speed of Nari was less than 3 m/s in average during landfall period, thus, should not alter the precipitation structure significantly. Under this weak vertical shear situation, the shift of the maximum rainfall rate from motion right front quadrant to motion ahead is consistent with that simulated by numerical model (Chen and Yau 2003). The model results suggested that the shift of maximum rainfall was due to the large difference of surface roughness length between ocean and land. The enhanced low level convergence produced by differential friction between ocean and land seems to play an important role of enhancing precipitation of a landfalling typhoon. After landfall, the maximum rainfall shifted to the motion rear quadrant in this case. This is because the enhanced precipitation induced by Taiwan topography was stationary with respect to storm movement. In this case it is difficult to distinguish between the effect of terrain slope uplifting and the enhanced convergence by

differential friction.

4. TRMM observations

During the landfall period of Nari, TRMM satellite made several overpasses. Fig.3 shows the reflectivity images of TRMM precipitation radar observations before and after landfall. It can be seen that while the storm was still in the open ocean, the maximum reflectivity occurred in motion right front quadrant and shifted to the motion right rear quadrant after it made landfall. It is worth to note that, however, the convective activity overall intensified significantly. In Fig.3, it also shows the vertical profiles of reflectivity of convective precipitation in the inner core (<100km) motion right front quadrant before and after landfall. The separation of convective and stratiform precipitation followed the technique developed by Steiner et al. (1995). There were 42 pixels satisfy the criteria before landfall and 75 pixels after landfall. The reflectivity profiles show large differences in intensity, before landfall the largest value is 42 dBZ and after landfall was 50 dBZ. Convert these reflectivity values to rainfall rates using $Z=300R^{1.4}$, they are 14.5 and 63.4

mmh⁻¹, respectively, a dramatic rainfall intensity change. This observation was consistent with what was observed by NEXRAD discussed in the previous section.

It is interesting to point out that extreme low brightness temperature also detected by TRMM 85GHz TMI sensor. Before landfall, the lowest polarization corrected temperature (PCT, defined by Spencer et al. 1989) was 220K, however, after landfall, PCT less than 180K was detected (figure not shown). According to Mohr and Zipser (1996), when PCT is less than 200K, it means there are large amount of precipitation-size ice particles existed in the cloud and significant lightning activity is anticipated. From both the ground surface station observation record and TRMM lightning mapper, all these observations confirmed the existence of lightning and indicated the occurrence of deep thunderstorms during the landfall period of typhoon Nari. Deep convection development in a landfall tropical cyclone was recently documented by Geerts et al. (2000) when hurricane Georges (1998) made landfall in the Dominican Republic. The severe thunderstorm developed within the eye while the storm encountered the high mountain Cordillera Central. In Typhoon Nari case, the thunderstorm developed along the coastal region instead of the high mountain and was outside the eye wall region. These differences suggest possibly different triggering mechanisms were operated and deserve further investigation.

5. Summary

In this study, the precipitation structure of Typhoon Nari (0116) before and after landfall is examined using the reflectivity and brightness temperature data collected by NEXRAD in northern Taiwan and TRMM TMI and PR. Pronounced precipitation structure change was identified during this period. The contraction of the eye and the associated intensification of precipitation in the inner core region were observed and this phenomenon can be traced back to 4-5 hours before the storm made landfall. The final hour enhancement of precipitation (about 50% increases) before landfall suggested that the strengthening low level convergence induced by the differential friction may play important role. Since the mean vertical shear was rather weak for the whole period, the asymmetrical distribution of precipitation of the storm in the open ocean was consistent with that

expected from asymmetric boundary layer flow under a translating storm (Shapiro 1983). The change of the asymmetry during landfall can be crudely attributed to the effect of Taiwan topography. From TRMM observations, the detection of very low brightness temperature by 85GHz TMI and significant intensification of radar reflectivity by PR all suggested the existence of severe convective activity and this result is consistent with what was observed by NEXRAD in northern Taiwan.

Acknowledgement

This study is supported by National Science Council of Taiwan under the Grant NSC-91-2111-M-002-023-AP4. The help of Zhou Kun in TRMM data processing and figure drafting is acknowledged.

Reference

- Chen, Y. and M. K. Yau, 2003: Asymmetric structures in simulated landfalling hurricane. *J. Atmos. Sci.*, 60, 2294-2312.
- Corbosiero, K. and J. Molinari, 2002: The effect of vertical wind shear on the distribution of convection in tropical cyclones. *Mon. Wea. Rev.*, 130, 2110-2123.
- Geerts, B., G. M. Heymsfield, L. Tian, J. B. Halverson, A. Guillory, and M. I. Mejia, 2000: Hurricane Georges's landfall in the Dominican Republic: Detailed airborne Doppler radar imagery. *Bull. Amer. Meteor. Soc.*, 81, 999-1018.
- Hanley, D. E., J. Molinari, and D. Keyser, 2001: A composite study of the interactions between tropical cyclones and upper tropospheric troughs. *Mon. Wea. Rev.*, 129, 2570-2584.
- Mohr, K. I., and E. J. Zipser, 1996: Defining mesoscale convective systems by their 85-GHz ice-scattering signatures. *Bull. Amer. Meteor. Soc.*, 77, 1179-1189.
- Rodgers, E. B., S. W. Chang, and H. F. Pierce, 1994: A satellite observational and numerical study of precipitation characteristics in western north Atlantic tropical cyclones. *J. Appl. Meteor.*, 33, 129-139.
- Shapiro, L. J., 1983: The asymmetric boundary layer flow under a translating hurricane. *J. Atmos. Sci.*, 40, 1984-1998.
- Spencer, R. W., H. M. Goodman, and R. E. Hood, 1989: Precipitation retrieval over land and ocean with the SSM/I: identification and characteristics of scattering signal. *J. Atmos. Oceanic Technol.*, 6, 254-273.
- Steiner, M., R. A. Houze Jr., and S. E. Yuter, 1995: Climatological characterization of three-dimensional storm structure from operational radar and rain gauge data. *J. Appl. Meteor.*, 34, 1978-2007.